

Perturbation of BRD4 Protein Function by BRD4-NUT Protein Abrogates Cellular Differentiation in NUT Midline Carcinoma^{*[5]}

Received for publication, April 2, 2011, and in revised form, June 7, 2011. Published, JBC Papers in Press, June 7, 2011, DOI 10.1074/jbc.M111.246975

Junpeng Yan, Jason Diaz, Jing Jiao, Ranran Wang, and Jianxin You¹

From the Department of Microbiology, University of Pennsylvania Perelman School of Medicine, Philadelphia, Pennsylvania 19104

NUT midline carcinoma (NMC) belongs to a class of highly lethal and poorly differentiated epithelial cancers arising mainly in human midline organs. NMC is caused by the chromosome translocation-mediated fusion of the *NUT* (nuclear protein in testis) gene on chromosome 15 to a few other genes, most frequently the *BRD4* gene on chromosome 19. The mechanism by which the *BRD4-NUT* fusion product blocks NMC cellular differentiation and contributes to oncogenesis remains elusive. In this study, we show that BRD4-NUT and BRD4 colocalize in discrete nuclear foci that are hyperacetylated but transcriptionally inactive. BRD4-NUT recruits histone acetyltransferases to induce histone hyperacetylation in these chromatin foci, which provide docking sites for accumulation of additional BRD4 and associated P-TEFB (positive transcription elongation factor b) complexes in the transcriptionally inactive BRD4-NUT foci. These molecular events lead to repression of a BRD4-P-TEFB downstream target gene *c-fos*, a component of activator protein 1 (AP-1), that directly regulates epithelial differentiation. Knockdown of *BRD4-NUT* in NMC cells disperses the transcriptionally inactive chromatin foci and releases the transcriptional activators to stimulate *c-fos* expression, leading to restoration of cellular differentiation. Our study provides a novel mechanism by which the *BRD4-NUT* oncogene perturbs BRD4 functions to block cellular differentiation and to contribute to the oncogenic progression in the highly aggressive NMC.

The aberrant activity of fusion products derived from chromosomal translocations as a mediator of oncogenesis has been well established in many forms of cancers, especially of the hematopoietic system (1). Their importance in carcinomas only started to be appreciated about a decade ago and has been shown to underlie certain prostate and lung cancers (2–4). Fusion proteins can cause aberrant functions through a variety of mechanisms, including increased or decreased expression of key oncogenes or tumor suppressors, aberrant cellular localization, altered stability of otherwise normal protein products, or

the incorrect expression of a gene not normally expressed in the affected cells.

NMC² is a rare but highly lethal and poorly differentiated or undifferentiated epithelial cancer caused by genetic translocations that lead to the fusion of the *NUT* gene on chromosome 15 to a few other genes (5). Among these, the most frequently occurring target is the *BRD4* gene on chromosome 19 (6, 7). *BRD4* is expressed normally as naturally occurring long (BRD4) and short (BRD4S) isoforms with identical 5' ends. Both *BRD4* transcripts encode the N-terminal double bromodomains and extra terminal domain, whereas the long *BRD4* transcript (amino acids 1–1362) encodes the C-terminal proline-rich and glutamine-rich regions that are absent in the *BRD4S* transcript (amino acids 1–722) (5, 6). The t(15;19) translocation breakpoint bisects *BRD4* at amino acid 719, while leaving the *BRD4S* unperturbed (5, 6). This translocation results in the novel in-frame fusion of the *BRD4* N-terminal component (amino acids 1–719) with nearly the entire sequence of *NUT* (amino acids 6–1132) (6).

BRD4 binds to acetylated chromatin through its bromodomains and becomes associated with both interphase chromatin and mitotic chromosomes (8). It plays a central role in cellular growth control and cell cycle progression (9–16). BRD4 also interacts with P-TEFB (composed of the CDK9-cyclin T1 dimer) via its extreme C-terminal domain that is absent in *BRD4S*. BRD4 binding reconstitutes the active form of P-TEFB, which phosphorylates serine 2 of the C-terminal domain (CTD) of RNA polymerase II (RNAP II) along the chromatin template, and stimulates transcriptional elongation (17, 18). In addition, BRD4 was found to contribute to the genome maintenance of some DNA tumor viruses during latent infection (19–21) and to be implicated in transcriptional regulation of a number of viral genomes (22–28). In contrast to *BRD4*, the function of the *NUT* gene is poorly understood, and its expression is restricted to the testis. The aberrant expression of *NUT* upon fusion to the *BRD4* moiety has been proposed as the defining feature of t(15;19) translocation-associated carcinoma (6).

There are more than 20 cases of NMC that have been identified (29–35). All of the known t(15;19)-positive NMCs were rapidly metastasizing and extremely aggressive (6). Identical *BRD4-NUT* fusion transcripts have been described in pediatric head and neck tumors (6) as well as in lung cancers (7). It has

* This work was supported, in whole or in part, by National Institutes of Health HIV-associated Malignancies Pilot Project Award from NCI and Grants R01CA148768 and R01CA142723.

[5] The on-line version of this article (available at <http://www.jbc.org>) contains supplemental Figs. S1–S9 and Table S1.

¹ To whom correspondence should be addressed: Dept. of Microbiology, University of Pennsylvania Perelman School of Medicine, 3610 Hamilton Walk, Philadelphia, PA 19104. Tel.: 215-573-6781; Fax: 215-898-9557; E-mail: jianyou@mail.med.upenn.edu.

² The abbreviations used are: NMC, NUT midline carcinoma; CTD, C-terminal domain; RNAP, RNA polymerase; CBP, cAMP-response element-binding protein-binding protein; HAT, histone acetyltransferase; qPCR, quantitative PCR.

Perturbation of BRD4 Function in BRD4-NUT Carcinoma Cells

been shown that BRD4-NUT could contribute to oncogenesis by blocking epithelial cell differentiation while promoting proliferation (36). Reynoird *et al.* (37) reported that BRD4-NUT interacts with p300 to cause histone hyperacetylation at its cellular chromatin-binding sites, leading to sequestration of acetylated p53 and down-regulation of p53 target genes. A recent report also showed that a novel small molecule inhibitor could bind competitively to the bromodomains and displace the BRD4 fusion oncoprotein from chromatin, provoking squamous differentiation and growth arrest in BRD4-NUT NMC cell lines (38). However, the molecular mechanism by which BRD4-NUT blocks cellular differentiation and contributes to oncogenic progression in NMC remains elusive.

NMC cells normally express one copy of *BRD4-NUT* and one copy of wild type *BRD4* long isoform (6). The t(15;19) translocation deletes the C-terminal domain of BRD4, without affecting BRD4S. Given that both BRD4 and BRD4-NUT contain the double bromodomains that can bind to acetylated histones, we decided to investigate how the BRD4-NUT fusion may trigger structural and functional changes in BRD4, contributing to the oncogenic mechanism in the NMC cells. Our results show that BRD4-NUT and BRD4 colocalize in discrete nuclear foci that are hyperacetylated but transcriptionally inactive. BRD4-NUT recruits HAT enzymes through the NUT moiety to induce histone hyperacetylation, which results in recruitment of additional BRD4 and associated P-TEFB. These molecular events lead to active repression of a BRD4-P-TEFB downstream target gene *c-fos*, which is a component of AP-1 that directly regulates epithelial cellular differentiation markers such as involucrin and Keratin in response to environmental stimulation (39–41). The down-regulation of the AP-1 complex has been observed in other carcinomas and seems to be a common feature of tumorigenesis (42–46). Our studies thus support a model in which transcriptionally inactive BRD4-NUT foci inhibit the BRD4-P-TEFB complex to down-regulate *c-fos* expression, contributing to abrogation of cellular differentiation and NMC oncogenesis.

EXPERIMENTAL PROCEDURES

Recombinant Plasmid Construction—The cDNAs encoding BRD4-NUT protein and NUT (amino acids 6–1132) were PCR-amplified from a GFP-BRD4-NUT construct kindly provided by Dr. Thao P. Dang (Vanderbilt University) and subcloned into a pOZN vector carrying both FLAG and HA tags. The pOZN-hBRD4S and pCDNA4c-NLS-BRD4(1–470) (BD I/II) constructs have been described previously (47). GST fusion constructs encoding full-length NUT and NUT fragments (300N, 550N, 850N, 300C, 697C, 800C, 960C, 300–550, and 300–700) were generated by cloning the PCR-amplified coding fragments into the pGEX-6P-1 vector. All plasmid constructs were verified by DNA sequencing. pCMV-FLAG-CBP was kindly provided by Dr. Paul M. Lieberman (The Wistar Institute). pCDNA4c-BRD4 and pCDNA4c-BRD4(1047–1362) (CTD) were from our laboratory plasmid bank. pCDNA3-CDK9 and pCDNA3-cyclin T1-HA were generous gifts from Dr. Bassel E. Sawaya (Temple University).

Cell Culture, Transfection, siRNA, and Antibodies—The HCC2429 cells (provided by Dr. Thao P. Dang) were maintained as monolayers in RPMI 1640 medium (Invitrogen) sup-

plemented with 10% FBS (Hyclone) and 1% penicillin/streptomycin (Invitrogen). 293T, C33A, and A549 cells were maintained in Dulbecco's modified Eagle's medium (Invitrogen) containing 10% FBS and 1% penicillin/streptomycin. C33A cells were transfected at 40–50% confluency using FuGENE 6 (Roche Applied Science) following the manufacturer's instructions. 293T cells were transfected at 40–50% confluency using the calcium phosphate method as described previously (47). Cells were harvested at 48 h after transfection. Lipofectamine 2000 (Invitrogen) was used to transfect DNA constructs into HCC2429 cells at about 50% confluency. Cells were harvested 48 h after transfection. For siRNA transfections, either Dharmafect 1 (Dharmacon) or Lipofectamine RNAi Max (Invitrogen) was used to transfect HCC2429 cells at about 40% confluency following the manufacturer's instructions. The cells were harvested at the indicated times post-transfection as described in the figure legends.

The control and *NUT* siRNAs were purchased from Dharmacon. The antibodies used in this study are as follows: anti-NUT (3625, Cell Signaling Technology); anti-acetyl-histone H4 (06-866, Millipore); anti-histone H3 (06-755, Millipore); anti-FLAGM2 (F3165, Sigma); anti-CDK9 (sc-484, Santa Cruz Biotechnology); anti-cyclin T1 (sc-8127, Santa Cruz Biotechnology); anti-GAPDH (G8140-01, US Biological); anti-involucrin (I 9081, Sigma); anti-RNAP II CTD serine 2 phosphorylation (ab5095, AbCAM); RNAP II monoclonal antibody sampler (MPY-127R, Covance); anti-HA-HRP (12013819001, Roche Applied Science); anti-Xpress (46–0528, Invitrogen); anti-AURORA A (610939, BD Biosciences); anti-AURORA B (611082, BD Biosciences); anti-GCN5 (07-1545, Millipore); anti-Tip60 (07-038, Millipore); and anti-cytokeratin AE1/AE3 (M3515, Dako).

Immunofluorescent Staining—Cells were grown on coverslips and fixed with 3% paraformaldehyde in PBS, incubated in blocking/permeabilization buffer (0.5% Triton X-100 and 3% BSA in PBS) for 10 min at room temperature, and stained with desired antibodies for 60 min. Cells were then washed three times with blocking/permeabilization buffer and incubated with Alexa Fluor-conjugated secondary antibodies (Molecular Probes) for another 60 min. In the case of double staining using two antibodies both derived from rabbit, each antibody was pre-labeled with Alexa Fluor 488- or Alexa Fluor 594-conjugated secondary antibody using Zenon rabbit IgG labeling kits (Z-25302 and Z-25307, Molecular Probes) following the manufacturer's instructions. The cells were incubated for 60 min with the pre-labeled antibodies and fixed in 4% paraformaldehyde for 15 min. Cells were counterstained with 4',6'-diamidino-2-phenylindole (DAPI) and examined using an Olympus IX81 inverted fluorescence microscope.

Immunoprecipitation, GST Pulldown, and HAT Assay—For anti-FLAG immunoprecipitation, cells were pelleted at 48 h post-transfection and resuspended in buffer A (10 mM HEPES (pH 7.9), 10 mM KCl, 0.1 mM EDTA, 0.1 mM EGTA, and 1 mM dithiothreitol (DTT) supplemented with protease inhibitors (Roche Applied Science)). The resuspended cells were incubated on ice for 10 min, and Nonidet P-40 was added to a final concentration of 0.6%. After vortexing and centrifugation at 5,000 rpm for 5 min, the nuclear pellet was resuspended in

ice-cold buffer B (20 mM HEPES (pH 7.9), 0.4 M NaCl, 1 mM EDTA, 1 mM EGTA, and 1 mM DTT, supplemented with protease inhibitors). To extract nuclear proteins, nuclei were passed through a 21-gauge needle five times and extracted at 4 °C for 1 h. Nuclear proteins were isolated by centrifugation at 14,000 rpm for 15 min, diluted in buffer A, mixed with 10 μ l of anti-FLAG M2-agarose beads (Sigma), and rotated at 4 °C overnight. The beads were washed three times with PBS containing 0.2 mM phenylmethylsulfonyl fluoride (PMSF) and used in the HAT assay.

For GST pulldowns, GST and GST-fused NUT fragments were expressed in *Escherichia coli* BL21(DE3)/pLysS and immobilized on glutathione-agarose beads following the manufacturer's protocol (Sigma). 20 μ l of GST or GST-NUT fragments immobilized on beads were incubated with 1.2 mg of 293T nuclear extracts at 4 °C overnight. Following three washes with PBS containing 0.2 mM PMSF, the beads were used in the HAT assay.

HAT assays were performed as follows. Immunoprecipitated and pulled down beads were pre-equilibrated with 500 μ l of 1 \times HAT buffer (50 mM Tris-Cl (pH 8.0), 0.1 mM EDTA (pH 8.0), 50 mM NaCl, 1 mM DTT, 10% glycerol, 1 mM PMSF, and 10 mM sodium butyrate supplemented with protease inhibitors). The other reagents were then added in the following order: 15 μ l of 2 \times HAT buffer, 10 μ g of histones (H9250, Sigma), 0.1 μ Ci of [¹⁴C]acetyl-CoA (PerkinElmer Life Sciences), and H₂O to a final volume of 30 μ l. The reaction was incubated at 30 °C for 1 h and stopped by adding 6 μ l of 6 \times SDS sample buffer and boiling for 5 min. In the case of nuclear extract HAT assays, beads were substituted with 40 μ g of nuclear extracts in the HAT reaction. Samples were resolved on SDS-PAGE and processed for autoradiography.

Reverse Transcription-Quantitative PCR (RT-qPCR)—HCC2429 cells were transfected with either NUT siRNA#1 or control siRNA. Total RNA was isolated at the indicated times post-transfection using TRIzol reagent (Invitrogen) following the manufacturer's instructions. Reverse transcription was performed in a 20- μ l reaction system containing 350 ng of total RNA using oligo(dT) primer (Invitrogen) and SuperScript II reverse transcriptase (Invitrogen) following the manufacturer's instructions. Real time PCR using gene-specific primers was performed in triplicate using 1 μ l of RT product in a 25- μ l reaction containing 12.5 μ l of iQ SYBR Green supermix (Bio-Rad) and 0.4 μ M of each primer. The reaction was carried out on a Bio-Rad iQTM 5 multicolor real time PCR detection system (Bio-Rad). The data were analyzed using Bio-Rad iQ5 software, and mRNA of each gene was normalized to GAPDH mRNA level. Primer sequences are shown in [supplemental Table S1](#).

ChIP Assay—HCC2429 cells were transfected with siRNA by Lipofectamine RNAi Max. At 27 h post-transfection, cells were harvested, and chromatin was prepared. ChIP assay was performed as described previously (47). Briefly, 100 μ g of chromatin was incubated with 2.5 μ g of normal rabbit IgG, H4ac, BRD4C, or RNAP II CTD serine 2 phosphorylation (Ser(P)-2) antibody at 4 °C for 14 h. After recovery of immune complexes, de-cross-linking of chromatin, phenol/chloroform extraction, and ethanol precipitation, DNA was resuspended in 20 μ l of H₂O. qPCR was performed as described above using primers

specifically amplifying the proximal promoter region of the indicated genes. 1 μ l of immunoprecipitated DNA or 1 μ l of 1:200 diluted total input chromatin was added as template in each PCR. Signal from each immunoprecipitated sample was normalized to input signal.

Image Quantitation—Immunofluorescent images were analyzed using ImageJ software. The "Adjust Threshold" function of the ImageJ software was used to identify BRD4, H4ac, CDK9, and cyclin T1 foci. Foci number and total foci intensity in each cell were analyzed using the "Analyze Particles" function of the software. The foci number and intensity in 40 BRD4-NUT-positive and 40 neighboring BRD4-NUT-negative cells from three biological repeats were measured. Results were plotted for both BRD4-NUT knockdown and overexpression experiments.

RESULTS

BRD4-NUT Recruits BRD4 to Speckled Nuclear Foci—The NMC cell line HCC2429 established from a t(15;19) BRD4-NUT translocation lung cancer patient was used in this study (7). As shown in Fig. 1A, the BRD4-NUT fusion protein can be detected in HCC2429 cells but not in A549 (human lung adenocarcinoma) cells (Fig. 1A, *BRD4-NUT blot*). In addition to BRD4-NUT, BRD4 protein could be detected in HCC2429 cells just as in A549 cells (Fig. 1A, *BRD4 blot*), confirming the presence of the wild type BRD4 allele in HCC2429 cells. Because BRD4 and BRD4-NUT both carry the double bromodomains that can bind to acetylated histones on chromatin, we first investigated if the BRD4-NUT fusion is able to compete with BRD4 for chromatin binding or if both proteins can colocalize on cellular chromatin in HCC2429 cells. To distinguish the full-length BRD4 from BRD4-NUT and BRD4S proteins, we generated a rabbit polyclonal antibody (named BRD4C) to specifically recognize the extreme C terminus of BRD4 (amino acids 1313–1362) but not BRD4-NUT and BRD4S. We also utilized siRNA targeting the NUT component of the fusion gene to specifically knock down the BRD4-NUT protein without affecting BRD4. BRD4-NUT and BRD4 were examined by immunofluorescent staining using NUT-specific antibody and BRD4C antibody that were prelabeled with Alexa Fluor 488 goat anti-rabbit and Alexa Fluor 594 goat anti-rabbit secondary antibodies, respectively. As shown in Fig. 1B, *top panel*, in control siRNA treated HCC2429 cells, BRD4-NUT forms punctate foci exclusively in the nucleus. This chromatin association of BRD4-NUT can be abrogated by a dominant negative inhibitor, the double bromodomains of BRD4, confirming the association of BRD4-NUT with cellular chromatin through its bromodomains ([supplemental Fig. S1](#)). The BRD4 staining also appears as punctate foci and clearly colocalizes with BRD4-NUT (Fig. 1B, *top panel*). In NUT siRNA#1-treated HCC2429 cells, BRD4-NUT was knocked down completely in about 50% of the cells. The field shown in Fig. 1B, *KD panel*, displays cells with no BRD4-NUT knockdown as well as cells with BRD4-NUT knockdown. As indicated by the arrow in the Fig. 1B, *KD panel*, BRD4-NUT knockdown leads to the disappearance of BRD4-NUT foci in these cells. Interestingly, BRD4 is also dispersed from the chromatin foci in all the BRD4-NUT knockdown cells (Fig. 1B, *bottom panel*). As shown in the ImageJ quantification results (Fig. 1B, *plots*), BRD4 foci number and intensity in

Perturbation of BRD4 Function in BRD4-NUT Carcinoma Cells

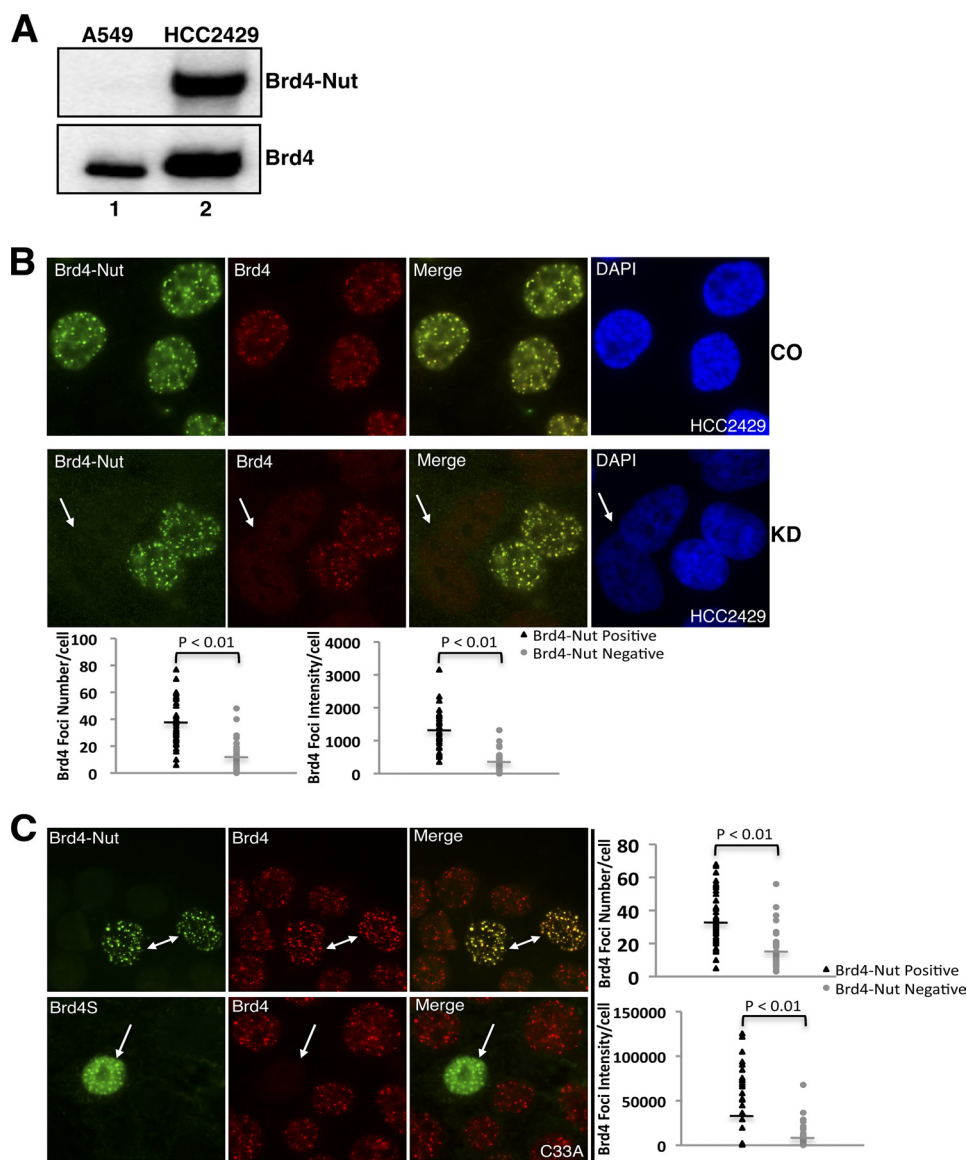


FIGURE 1. BRD4-NUT recruits BRD4 to speckled nuclear foci. *A*, A549 and HCC2429 cell lysates were analyzed by Western blot using NUT antibody (*BRD4-NUT*) or BRD4C antibody (*BRD4*). *B*, HCC2429 cells were transfected with control siRNA (CO) or siRNA#1 specifically targeting *NUT* (KD). Endogenous BRD4-NUT and BRD4 proteins were visualized by immunofluorescent staining using NUT antibody (BRD4-NUT) and BRD4C (BRD4) antibodies pre-labeled with Alexa Fluor 488 goat anti-rabbit and Alexa Fluor 594 goat anti-rabbit secondary antibodies, respectively. Cells were also counterstained with DAPI. The arrow indicates BRD4-NUT knockdown cells. The BRD4 foci number and intensity in cells treated with *BRD4* siRNA#1 were quantitated as described under "Experimental Procedures." The plots show the BRD4 foci number and intensity in BRD4-NUT-positive cells and neighboring BRD4-NUT-negative cells. The bars represent the average value of 40 cells from three biological repeats. *C*, C33A cells were transfected with FLAG-tagged BRD4-NUT (top panel) or BRD4S (bottom panel) expression constructs. Ectopically expressed proteins and endogenous BRD4 were detected by immunofluorescent staining using anti-FLAG antibody and BRD4C antibody, respectively. Arrows indicate cells with ectopically expressed proteins. The BRD4 foci number and intensity in cells transfected with FLAG-tagged BRD4-NUT construct were quantitated and plotted as described under "Experimental Procedures."

BRD4-NUT knockdown cells were dramatically reduced compared with neighboring non-knockdown cells (Fig. 1*B*, bottom panel). This result suggests that BRD4-NUT is responsible for recruiting BRD4 to its targeted chromatin foci in HCC2429 cells.

To confirm our observation, a FLAG-tagged BRD4-NUT expression construct was transfected into C33A (a cervical cancer cell line), which does not express BRD4-NUT (supplemental Fig. S2). In C33A cells, BRD4 is normally detected as punctate nuclear dots. As detected by anti-FLAG immunofluorescent staining, BRD4-NUT also forms punctate nuclear foci that colocalize with BRD4 in all the positively

transfected cells as indicated by arrows in Fig. 1*C*, top panel. In BRD4-NUT-positive cells, we observed higher BRD4 foci immunofluorescent signals than in BRD4-NUT-negative cells. ImageJ quantification shows that the number and intensity of BRD4 foci in BRD4-NUT-positive cells are all significantly higher than in neighboring BRD4-NUT-negative cells (Fig. 1*C*, plots), suggesting that more BRD4 is recruited to the BRD4-NUT foci than in the nontransfected neighboring cells. As a control, C33A cells were also transfected with a construct encoding the short isoform of BRD4, BRD4S, which spans amino acids 1–719 of BRD4. In contrast to BRD4-NUT expression, the FLAG-tagged BRD4S expression does not lead to

BRD4 chromatin recruitment; rather, it disperses endogenous BRD4 from the punctate chromatin foci in all positively transfected cells (Fig. 1C, *bottom panel*). In 293T cells, BRD4 normally displays a much more diffused nuclear staining. BRD4-NUT expressed in 293T cells forms punctate nuclear dots and also causes accumulation of BRD4 in these nuclear foci ([supplemental Fig. S3, top panel](#)). Conversely, BRD4S expression causes partial dissociation of BRD4 from chromatin ([supplemental Fig. S3, bottom panel](#)). Because both BRD4-NUT and BRD4S can bind to acetylated histones through the double bromodomains, the fact that BRD4S is able to competitively dissociate BRD4 while BRD4-NUT recruits more BRD4 to the speckled nuclear foci suggests that this phenomenon is likely to be induced by the NUT moiety of the fusion protein.

BRD4-NUT Induces the Formation of Histone-hyperacetylated Nuclear Foci—Because BRD4 binds to acetylated histones through its double bromodomains, it is possible that histone acetylation at the BRD4-NUT foci is boosted to enhance BRD4 recruitment. To test if the histone acetylation is changed at BRD4-NUT foci, we used a *NUT*-specific siRNA to knock down the BRD4-NUT protein in HCC2429 cells. BRD4-NUT and total histone H4 acetylation (H4ac) were examined by immunofluorescent staining using NUT antibody and total H4ac antibody that were pre-labeled with Alexa Fluor 488 goat anti-rabbit and Alexa Fluor 594 goat anti-rabbit secondary antibodies, respectively. As shown in Fig. 2A, *top panel*, in control siRNA-treated HCC2429 cells, the H4ac staining appears as punctate foci, which clearly colocalize with BRD4-NUT as shown in the merged image. However, in BRD4-NUT knockdown cells (as indicated by *arrows* in Fig. 2A, *bottom panel*), H4ac signal is dispersed from the hyperacetylated foci. The quantification results show that both number and intensity of the hyperacetylated foci are dramatically reduced in BRD4-NUT knockdown cells (Fig. 2A, *plots*). This result suggests that BRD4-NUT causes the formation of histone-hyperacetylated foci at discrete nuclear regions where it binds chromatin. To test whether the formation of histone-hyperacetylated foci affects total cellular histone H4 acetylation levels, a Western blot analysis was performed. As shown in Fig. 2B, BRD4-NUT in HCC2429 is efficiently knocked down by *NUT* siRNA#1 and siRNA#3, with *NUT* siRNA#2 and siRNA#4 being less efficient (Fig. 2B, *BRD4-NUT blot*). However, there is no obvious change in cellular histone H4 acetylation levels between control and *NUT* siRNA-treated cells (Fig. 2B, *H4ac blot*). The histone H3 blot (Fig. 2B, *H3 blot*) is shown as a loading control. These data suggest that BRD4-NUT could cause accumulation of histone acetylation in specific nuclear foci either through recruiting HATs to stimulate local histone acetylation or reorganizing the chromatin to result in increased concentration of histone acetylation in the BRD4-NUT foci. Because of its high efficiency in BRD4-NUT knockdown, *NUT* siRNA#1 was used throughout this study.

To further investigate the BRD4-NUT-associated histone-hyperacetylated foci, BRD4-NUT-, BRD4S-, and NUT-expressing constructs were transfected in C33A cells. When the BRD4-NUT protein was expressed in C33A cells, BRD4-NUT colocalizes with histone hyperacetylated foci, which are not obvious in nontransfected neighboring cells (Fig. 2C, *top*

panel). The quantification results show that BRD4-NUT expression leads to a significant increase of the number and intensity of histone-hyperacetylated foci (Fig. 2C, *plots*). BRD4S also localizes to punctate nuclear foci as BRD4-NUT, whereas NUT shuttles between the nucleus and cytoplasm as has been shown previously (36). Nonetheless, neither BRD4S nor NUT causes the formation of histone hyperacetylation foci in any of the 50 positively transfected cells examined (Fig. 2C, *middle and bottom panels*). These results confirm the BRD4-NUT-specific induction of histone-hyperacetylated foci in its binding regions. Taken together, this study demonstrates that the fusion of NUT moiety to BRD4 is necessary and sufficient to cause the formation of histone hyperacetylated foci on chromatin. Given that BRD4 binds to acetylated histones, this study also suggests that the hyperacetylated histone foci induced by the BRD4-NUT fusion protein further recruits additional BRD4 to these foci.

NUT Protein Associates with HAT Enzymes—BRD4-NUT-induced histone hyperacetylation suggests that BRD4-NUT may recruit HAT enzymes to accomplish this function. To investigate this further, BRD4-NUT was knocked down in HCC2429 cells, and total nuclear HAT activity was assessed by an *in vitro* HAT assay. As indicated in the Fig. 3A autoradiograph, knockdown of BRD4-NUT reduces the total cellular HAT activity (Fig. 3A, *Autorad*). As a control, the Coomassie Brilliant Blue stain shows that similar amounts of substrate histones were used in each HAT reaction. The Western blot in Fig. 3A, *top panel*, confirms the knockdown of BRD4-NUT, with the GAPDH blot serving as the loading control. We also performed an immunoprecipitation-HAT (IP-HAT) assay to directly assess if any HAT activity could be associated with BRD4-NUT. FLAG-tagged BRD4-NUT, BRD4S, and NUT were expressed in 293T cells, and their associated immunocomplexes were precipitated and assayed for HAT activity. BRD4-NUT and NUT immunocomplexes show strong HAT activity, whereas BRD4S displays a similar background signal as seen in the vector control ([supplemental Fig. S4](#)). This experiment suggests that, in BRD4-NUT, the NUT domain could either possess intrinsic HAT activity or associate with other HATs. To distinguish between these possibilities, the NUT protein was fused to GST and expressed in *E. coli*. The HAT activity of the GST-NUT fusion was evaluated either with or without incubation with 293T nuclear extracts. As shown in Fig. 3B, there is no detectable HAT activity for either GST or GST-NUT proteins that were not incubated with nuclear extracts (Fig. 3B, *autorad., lanes 1 and 3*). However, the HAT activity can be detected after GST-NUT was incubated with 293T nuclear extracts (Fig. 3B, *autorad., lane 4*). No HAT activity can be detected for the GST protein after incubation with 293T nuclear extracts (Fig. 3B, *autoradiograph, lane 2*). This result suggests that the NUT protein does not have intrinsic HAT activity and that it associates with other HAT enzymes to induce histone hyperacetylation at the BRD4-NUT-specific nuclear foci. Further studies mapped the HAT association domain to the amino acid 300–550 region of the NUT protein ([supplemental Fig. S5](#)). In line with this finding, a recent report from Reynoird *et al.* shows that the NUT protein can interact with p300 through the F1c region spanning amino acid 346–593 of NUT protein (37). To deter-

Perturbation of BRD4 Function in BRD4-NUT Carcinoma Cells

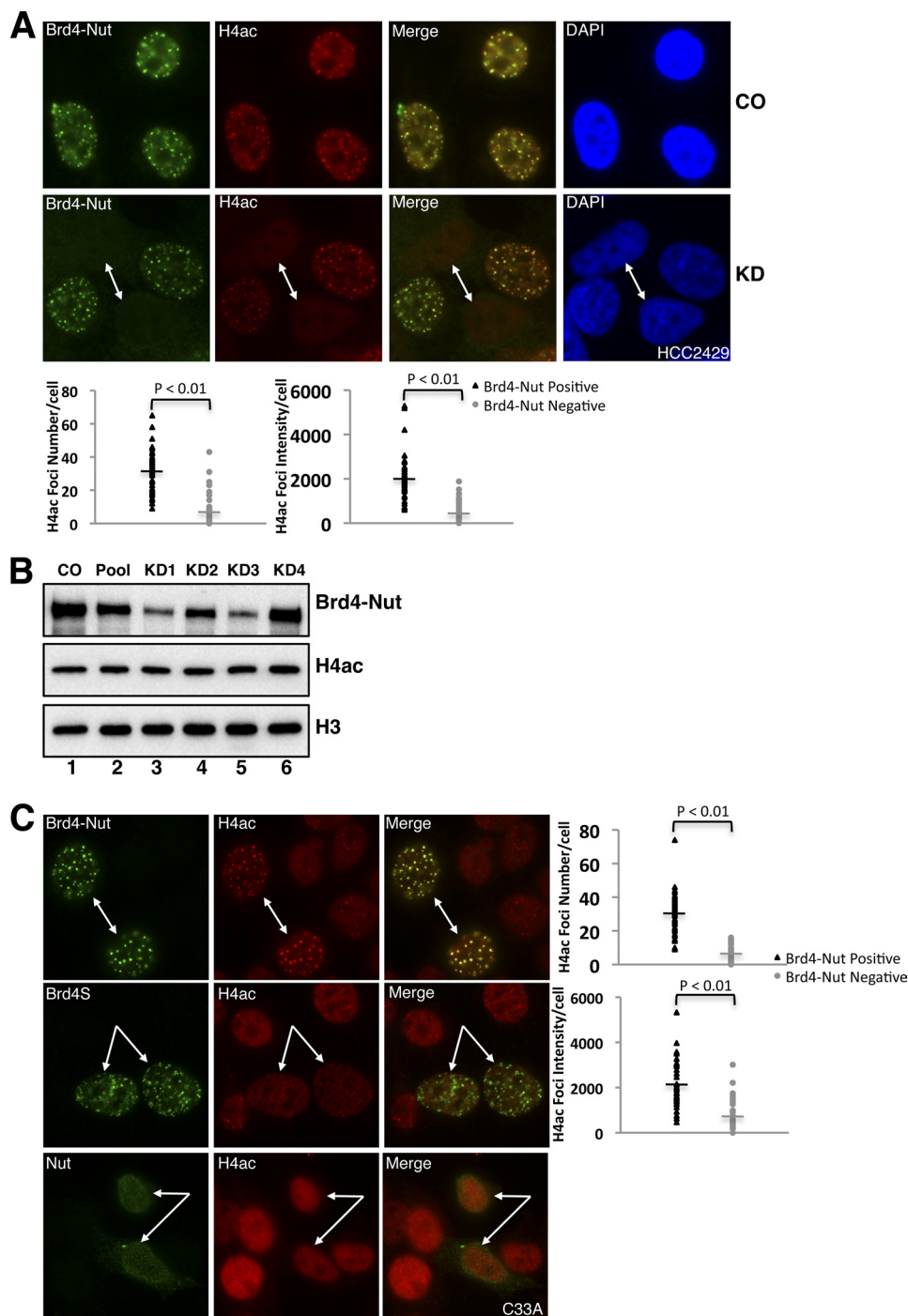


FIGURE 2. BRD4-NUT induces the formation of histone-hyperacetylated nuclear foci. *A*, HCC2429 cells were transfected with control siRNA (CO) or *NUT* siRNA#1 (KD). Endogenous BRD4-NUT protein and acetylated histone H4 were visualized by immunofluorescent staining using NUT antibody (BRD4-NUT) and total acetylated histone H4 antibody (H4ac) pre-labeled with Alexa Fluor 488 goat anti-rabbit and Alexa Fluor 594 goat anti-rabbit secondary antibodies, respectively. Cells were also counterstained with DAPI. Arrows indicate BRD4-NUT knockdown cells. The H4ac foci number and intensity in cells treated with BRD4 siRNA#1 were quantitated and plotted as described under "Experimental Procedures." *B*, HCC2429 cells were transfected with either nontargeting control siRNA (CO), individual siRNAs targeting *NUT* (KD1, KD2, KD3, and KD4, respectively), or the mixture of all four siRNAs (Pool). Cell lysates were analyzed by Western blot using NUT antibody (BRD4-NUT), acetyl-histone H4 antibody (H4ac), or histone H3 antibody (H3, as a loading control). *C*, C33A cells were transfected with FLAG-tagged BRD4-NUT (top panel), BRD4S (middle panel), or NUT (bottom panel) expression construct. Ectopically expressed proteins and acetylated histone H4 were detected by immunofluorescent staining using anti-FLAG antibody and total acetylated histone H4 antibody (H4ac). Arrows indicate BRD4-NUT-, BRD4S-, or NUT-expressing cells. The H4ac foci number and intensity in cells transfected with FLAG-tagged BRD4-NUT construct were quantitated and plotted as described under "Experimental Procedures."

mine whether other HAT enzymes may also interact with NUT and contribute to BRD4-NUT-mediated histone hyperacetylation, we tested a number of HATs, including MYST, GCN5, TIP60, and P/CAF for the ability to interact with NUT and

NUT(300–550) fragment. CBP and p300 were also included as positive controls. GST, GST-NUT, and GST-NUT(300–550) expressed in *E. coli* were immobilized on glutathione-agarose beads. After incubation with 293T nuclear extracts, bound pro-

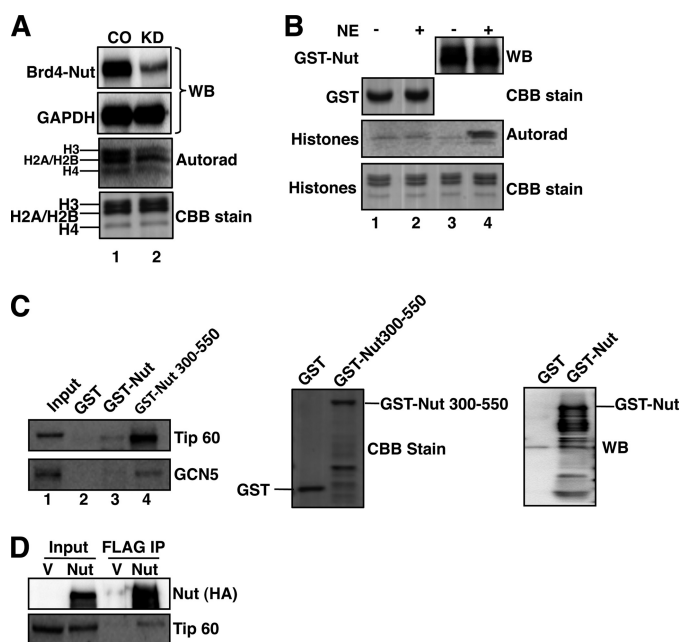


FIGURE 3. NUT protein associates with HAT activity. *A*, HCC2429 cells were transfected with control siRNA (CO) or *NUT* siRNA#1 (KD). Equal amounts of nuclear extracts were analyzed for HAT activity using [¹⁴C]acetyl-CoA and histones and visualized by autoradiography (*autorad*). 1/10 of HAT reactions were analyzed on SDS-PAGE and stained with Coomassie Brilliant Blue (CBB stain). Nuclear extracts were also analyzed by Western blot (WB) using NUT antibody (BRD4-NUT) and GAPDH antibody (GAPDH, serves as loading control) to verify knockdown of BRD4-NUT protein. Experiments were repeated two times with similar results. *B*, NUT was expressed as a GST fusion in *E. coli* and immobilized on glutathione-agarose beads. The beads were incubated with (+) or without (−) 293T nuclear extracts (NE) before the HAT assay. The HAT activity was detected by autoradiography (*autorad*). Western blot analysis was used to confirm the presence of GST-NUT protein. Coomassie Brilliant Blue stain (CBB stain) was used to visualize the GST protein and the amount of histones added into each HAT reaction. Shown are representative results from three independent experiments. *C*, immobilized GST, GST-NUT, or GST-NUT(300–550) was incubated with 293T nuclear extracts. Bound proteins were analyzed using Western blot with TIP60 or GCN5 antibodies (*left panel*). GST, GST-NUT, and GST-NUT(300–550) proteins eluted from the beads were visualized by Coomassie Brilliant Blue stain (*middle panel*) or Western blot using NUT antibody (*right panel*). *D*, NUT interacts with Tip60. 293T cells were transfected with empty vector (V) or pOZN-NUT (NUT). Nuclear extracts were prepared and incubated with FLAG M2 beads. Immunoprecipitates (IP) were analyzed using Western blot with HA (for NUT) and Tip60 antibodies.

teins were analyzed using Western blot with antibodies against specific HATs. The results show that, besides CBP and p300, TIP60 and GCN5 can also bind to both GST-NUT and GST-NUT(300–550) but not to the GST control (Fig. 3C and data not shown). The rest of the HAT enzymes tested show no significant interaction with either GST-NUT or GST-NUT(300–550). Both TIP60 and GCN5 bind more efficiently to the GST-NUT(300–550) than GST-NUT presumably because GST-NUT is expressed at a much lower level in *E. coli*. Using FLAG-tagged full-length NUT protein expressed in 293T cells, we can also coimmunoprecipitate endogenous TIP60 (Fig. 3D). This study demonstrates that, in addition to CBP and p300, NUT protein can interact with additional HAT enzymes such as TIP60 and GCN5 to induce the histone hyperacetylation on chromatin.

P-TEFB Is Recruited to Transcriptionally Inactive BRD4-NUT Nuclear Foci—BRD4 stimulates transcription by recruiting P-TEFB to phosphorylate the RNAP II CTD along the chromatin template. Recruitment of P-TEFB to the chromosome is

crucial for expression of BRD4 downstream genes (13, 15). Our observation that BRD4 is accumulated at BRD4-NUT nuclear foci in HCC2429 cells prompted us to test whether P-TEFB is also recruited to the BRD4-NUT nuclear foci through BRD4. In Fig. 4A, HCC2429 cells were transfected with *NUT* siRNA#1 to knock down BRD4-NUT. The cells were immunostained to detect the localization of BRD4-NUT as well as CDK9 and cyclin T1, the two components of P-TEFB. The fields shown in Fig. 4A contain a mixture of cells with no knockdown and knockdown of BRD4-NUT to allow comparison. Knockdown cells are marked with *arrows* in Fig. 4A. In HCC2429 cells that retain BRD4-NUT expression, both CDK9 (Fig. 4A, *top panel*) and cyclin T1 (*bottom panel*) colocalize with BRD4-NUT in the nuclear foci. However, in BRD4-NUT knockdown cells, the CDK9 and cyclin T1 foci are dispersed, and the signals of both P-TEFB subunits appear diffused (Fig. 4A). ImageJ quantification results show that both number and intensity of the P-TEFB foci are dramatically reduced in BRD4-NUT knockdown cells (Fig. 4A, *plots*). This result suggests that BRD4-NUT can partially sequester P-TEFB to its target binding sites on chromatin and that knockdown of BRD4-NUT can release the P-TEFB from these chromatin foci. To test this further, the BRD4-NUT protein was expressed in C33A cells. P-TEFB subunits are now recruited to the BRD4-NUT nuclear foci in the BRD4-NUT expressing C33A cells (Fig. 4B). P-TEFB foci number and intensity are significantly increased in BRD4-NUT-expressing C33A cells compared with neighboring BRD4-NUT-negative cells (Fig. 4B, *plots*). In addition, expression of the BRD4 C-terminal domain (spanning BRD4 amino acids 1047–1362), which contains the P-TEFB interacting region and functions as a dominant negative inhibitor to block BRD4-P-TEFB interaction, can disperse P-TEFB nuclear foci in HCC2429 cells (*supplemental Fig. S6*). From these results we concluded that P-TEFB is partially recruited to BRD4-NUT nuclear foci in HCC2429 cells through binding to BRD4.

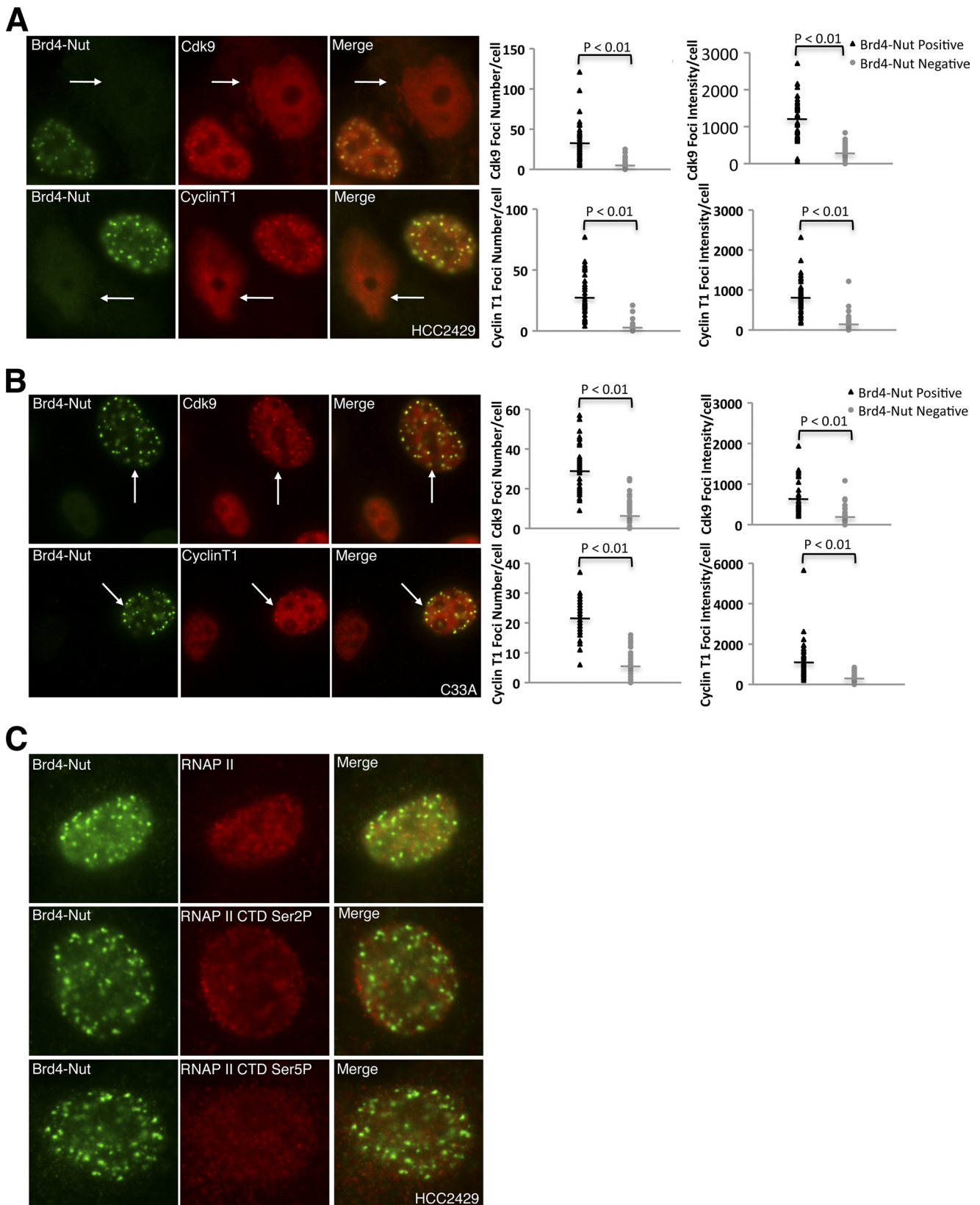
Because it has been well established that, when complexed with BRD4, P-TEFB stimulates transcriptional elongation by phosphorylating the serine 2 residue of the RNAP II CTD, we wondered whether the BRD4-P-TEFB complex accumulated in BRD4-NUT foci is transcriptionally active. To test this, HCC2429 cells were examined by immunofluorescent staining to detect BRD4-NUT, RNAP II, and two markers of active transcription, RNAP II CTD Ser(P)-2 and RNAP II CTD Ser(P)-5. As shown in Fig. 4C, RNAP II, RNAP II CTD Ser(P)-2, and RNAP II CTD Ser(P)-5 signals are all excluded from the BRD4-NUT foci, and no colocalization can be detected for BRD4-NUT and the active transcription markers in the 50 cells examined in each case. This result suggests that enrichment of HATs, hyperacetylated histones and the BRD4-P-TEFB complexes at the BRD4-NUT foci does not activate transcription in these chromatin regions.

BRD4-NUT Blocks NMC Cellular Differentiation by Inhibition of *c-fos* Transcription—NMC is currently diagnosed as a poorly differentiated or undifferentiated cancer (5). BRD4-NUT knockdown in HCC2429 cells induces characteristic morphological changes, including increased cellular cohesion, stratification, flattening, and enlargement of the cells, indicating the induction of squamous differentiation in this cell line

Perturbation of BRD4 Function in BRD4-NUT Carcinoma Cells

(supplemental Fig. S7) (36). In addition, BRD4-NUT knock-down-induced cellular differentiation also caused inhibition of HCC2429 cell proliferation (supplemental Fig. S8). To establish a functional link between BRD4-NUT and cellular differentia-

tion, we adopted a widely used marker, involucrin, to evaluate cellular differentiation upon BRD4-NUT knockdown in HCC2429 cells (39). In Fig. 5A, HCC2429 cells were transfected with either control siRNA (CO) or *NUT* siRNA#1 (*KD*). Total



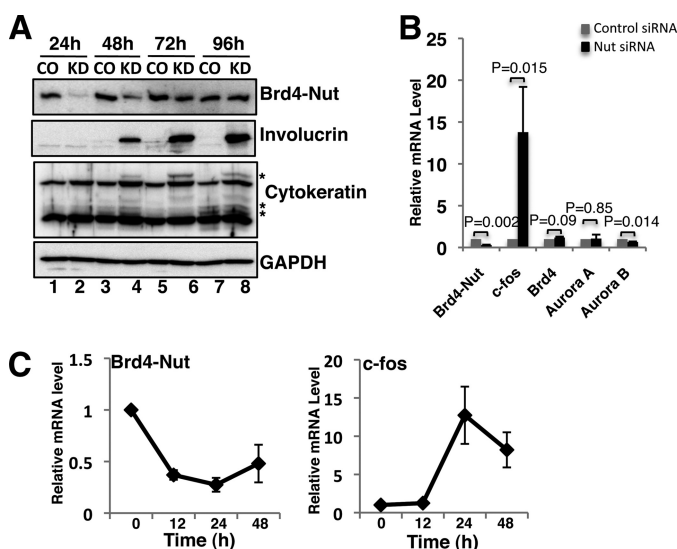


FIGURE 5. BRD4-NUT blocks NMC cellular differentiation by inhibiting *c-fos* transcription. *A*, HCC2429 cells were transfected with control siRNA or *NUT* siRNA#1 by Lipofectamine RNAi Max. Cells were harvested and lysed at indicated times post-transfection. Total cell lysates were resolved on SDS-PAGE and analyzed using indicated antibodies in Western blot. *B*, HCC2429 cells were transfected with control siRNA or *NUT* siRNA#1. Total RNA was extracted at 24 h post-transfection. Relative mRNA levels of selected genes were measured by RT-qPCR and normalized to the GAPDH mRNA level. Values represent the average of three independent experiments with error bars indicating standard deviation. *C*, HCC2429 cells were treated with siRNAs described in *B*. RNA extraction and RT-qPCR were performed at indicated times post-transfection. The mRNAs of *BRD4-NUT* and *c-fos* were normalized to GAPDH mRNA levels and presented as the ratio of transcript in knockdown sample relative to control sample at each time point. Values represent the average of three independent experiments with error bars indicating standard deviation.

cell lysates were analyzed by Western blot. BRD4-NUT protein levels dropped dramatically starting at 24 h post-transfection (Fig. 5A, *BRD4-NUT blot*, compare lane 2 with lane 1). At 48 h after siRNA transfection, BRD4-NUT protein was still efficiently knocked down, and we detected strong induction of involucrin in BRD4-NUT knockdown cells (Fig. 5A, compare lane 4 with lane 3), indicating an induction of cellular differentiation. At 72 h and 96 h post-transfection, although BRD4-NUT protein recovered gradually in knockdown cells due to the alleviation of siRNA effect, cells continued to differentiate as indicated by the continuous induction of involucrin. In addition to involucrin, another cellular differentiation marker, cytokeratin, was also specifically induced upon BRD4-NUT knockdown (Fig. 5A, *cytokeratin blot*, asterisks mark the cytokeratin bands induced by BRD4-NUT knockdown). The *GAPDH blot* in Fig. 5A is included as a loading control. This result demonstrates that knockdown of BRD4-NUT leads to an irreversible differentiation of NMC cells, supporting the notion

that BRD4-NUT functions as a major block for HCC2429 cellular differentiation.

Previous studies have shown that *c-fos*, a component of the AP-1 complex, is the immediate upstream regulator of cellular differentiation markers and is required for normal epithelial cell differentiation (39–41). It has also been shown that the *c-fos* gene is regulated by the BRD4·P-TEFB complex (48, 49). Because the BRD4·P-TEFB complex is recruited to transcriptionally inactive BRD4-NUT foci (Figs. 1 and 4), we hypothesized that this may lead to down-regulation of the *c-fos* gene and inhibition of cellular differentiation in NMC. To address this question, we first performed RT-qPCR to compare the mRNA levels of *c-fos* in HCC2429 cells treated with either control or *NUT* siRNA#1 (Fig. 5B). As a comparison, we also examined a few other genes, including both BRD4 downstream targets such as *AURORA B* and BRD4-independent genes such as *AURORA A* (16). In cells treated with *NUT*-specific siRNA, the BRD4-NUT mRNA levels dropped to 30% of the control level (Fig. 5B). In the meantime, *c-fos* mRNA was dramatically increased upon BRD4-NUT knockdown (Fig. 5B). In contrast, the mRNA levels of *BRD4* and *AURORA A* were not affected with *AURORA B* mRNA reduced to 67% when BRD4-NUT was knocked down (Fig. 5B). In a time course measurement of *c-fos* and *BRD4-NUT* mRNA in HCC2429 cells after *NUT* siRNA#1 treatment, we observed that *BRD4-NUT* mRNA drops about 63% at 12 h post-transfection, whereas *c-fos* mRNA remains constant during this time period (Fig. 5C). However, *c-fos* mRNA increases ~13-fold when the *BRD4-NUT* mRNA is reduced about 75% at 24 h post-transfection (Fig. 5C). Although the *BRD4-NUT* mRNA level remains low until 48 h post-transfection, *c-fos* mRNA induction is reduced from 13- to about 8-fold at this time point (Fig. 5C). This result indicates that *c-fos* gene transcription was induced transiently by BRD4-NUT knockdown. Taken together, these results demonstrate the induction of *c-fos* mRNA by BRD4-NUT knockdown and suggest that BRD4-NUT blocks NMC cellular differentiation, at least in part, through repression of the *c-fos* transcription.

BRD4-NUT Knockdown Restores Histone Acetylation and BRD4·P-TEFB Recruitment on *c-fos* Promoter—As described above, BRD4-NUT knockdown leads to the dispersion of the histone-hyperacetylated nuclear foci and release of BRD4 and P-TEFB. We next examined if the BRD4-NUT knockdown-induced *c-fos* transcription is due to the release of these transcriptional activators from BRD4-NUT foci. Chromatin immunoprecipitation (ChIP) was performed to compare the presence of transcriptional activators on the *c-fos* proximal promoter region in control and *NUT* siRNA#1-transfected HCC2429 cells. We observed increases of H4ac and BRD4 on the *c-fos*

FIGURE 4. P-TEFB is recruited to transcriptionally inactive BRD4-NUT nuclear foci. *A*, HCC2429 cells were transfected with *NUT* siRNA#1. Endogenous BRD4-NUT and CDK9 proteins were visualized with NUT antibody, and CDK9 antibody was labeled with Alexa Fluor 488 goat anti-rabbit and Alexa Fluor 594 goat anti-rabbit secondary antibodies, respectively (top panel). Endogenous BRD4-NUT and cyclin T1 proteins were detected using NUT antibody and cyclin T1 antibody by immunofluorescent staining. Arrows indicate knockdown cells. The CDK9 and cyclin T1 foci number and intensity in cells treated with *NUT* siRNA#1 were quantitated and plotted as described under “Experimental Procedures.” *B*, C33A cells were transfected with FLAG-tagged BRD4-NUT expression constructs. Ectopically expressed proteins were detected by anti-FLAG antibody. P-TEFB was detected using either CDK9 antibody (top panel) or cyclin T1 antibody (bottom panel) by immunofluorescent staining. Arrows indicate BRD4-NUT expressing cells. The CDK9 and cyclin T1 foci number and intensity in cells transfected with FLAG-tagged BRD4-NUT construct were quantitated and plotted as described under “Experimental Procedures.” *C*, endogenous BRD4-NUT in HCC2429 cells was visualized together with RNAP II (top panel), RNAP II CTD serine 2 phosphorylation (*RNAP II CTD Ser2P*, middle panel) or RNAP II CTD serine 5 phosphorylation (*RNAP II CTD Ser5P*, bottom panel) by immunofluorescent staining. More than 50 cells from three biological repeats were examined, and no colocalization of BRD4-NUT with RNAP II, RNAP II CTD Ser(P)-2, or RNAP II CTD Ser(P)-5 was observed.

Perturbation of BRD4 Function in BRD4-NUT Carcinoma Cells

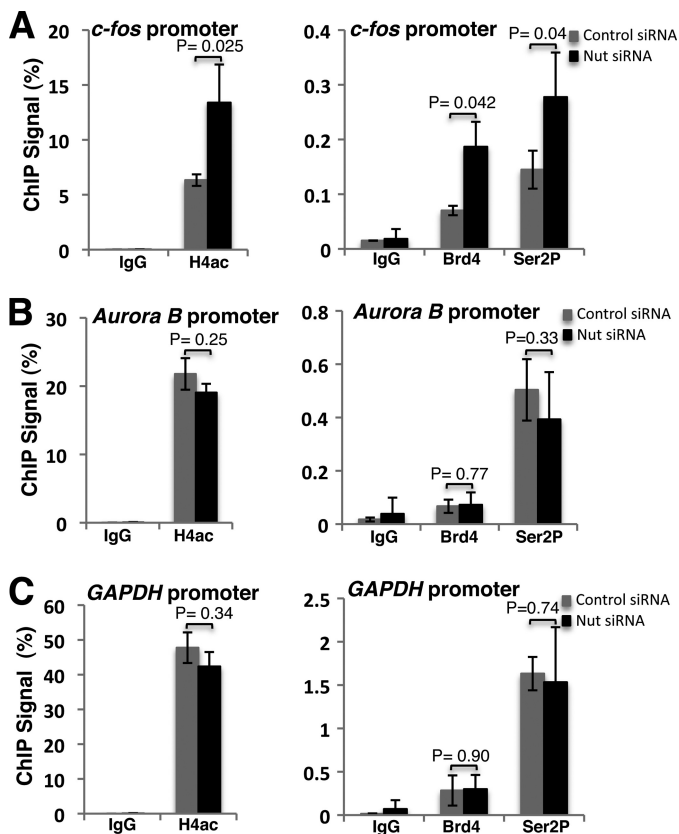


FIGURE 6. BRD4-NUT knockdown restores histone acetylation and BRD4-P-TEFB recruitment on *c-fos* promoter. ChIP analysis was performed using control siRNA or NUT siRNA#1-treated HCC2429 cells. Chromatin was precipitated with normal rabbit IgG (IgG, as control), acetyl-histone H4 (H4ac), BRD4C (BRD4), or RNAP II CTD serine 2 phosphorylation (Ser2P) antibodies. Precipitated chromatin was analyzed for the proximal promoter regions of *c-fos* (A), *AURORA B* (B), and *GAPDH* (C) gene using qPCR and presented as percentage of input. Values represent the average of three independent experiments with error bars indicating standard deviation.

promoter when BRD4-NUT is knocked down (Fig. 6A). To measure the P-TEFB activity on the *c-fos* promoter, we tested RNAP II CTD serine 2 phosphorylation and found that it is also significantly increased upon BRD4-NUT knockdown (Fig. 6A). In contrast, H4ac, BRD4, and Ser(P)-2 levels remain unchanged on *AURORA B* and *GAPDH* promoters upon BRD4-NUT knockdown (Fig. 6, B and C). Additionally, there is no obvious change in total cellular BRD4 and P-TEFB protein levels when BRD4-NUT was knocked down in HCC2429 cells (supplemental Fig. S9). In conclusion, our result suggests that BRD4-NUT knockdown releases transcriptional activators from BRD4-NUT foci and allows them to relocate to the *c-fos* promoter for transcriptional activation, leading to induction of NMC cellular differentiation.

Expression of CBP and BRD4-P-TEFB Stimulates c-fos Transcription and Cellular Differentiation in NMC Cells—To further examine the sequestration of transcriptional activators by BRD4-NUT foci, we tested if expression of these transcriptional activators could reverse the sequestration effects and promote *c-fos* transcription as well as cellular differentiation in HCC2429 cells. BRD4, CDK9, cyclin T1, and CBP, a HAT that has been shown to be sequestered at the BRD4-NUT foci (37), were included in this study. These molecules were individually

expressed in HCC2429 cells. As shown in Fig. 7, A and C, *c-fos* mRNA is dramatically increased in cells transfected with CBP and BRD4 compared with the empty vector controls; CDK9 expression leads to about 2-fold induction of *c-fos* mRNA, whereas cyclin T1 only slightly increases *c-fos* transcription. However, *AURORA A* and *AURORA B* mRNA levels are not affected by any of the expressed proteins (Fig. 7, A and C). These results suggest that the expression of CBP, BRD4, and P-TEFB can alleviate BRD4-NUT-mediated sequestration of transcriptional activators and in turn stimulate the *c-fos* gene expression in NMC cells. To further evaluate the cellular differentiation status upon expression of these transcriptional activators, Western blotting was performed to assess the involucrin level. With expression of CBP and BRD4, strong induction of involucrin is observed compared with the vector controls (Fig. 7, B and D, compare lane 2 with lane 1). Compared with the vector control, a small induction of involucrin can also be detected in CDK9 and cyclin T1-transfected cells (Fig. 7D, involucrin blot, compare lanes 3 and 4 with lane 1). As controls, *AURORA A* and *AURORA B* protein levels are not affected by any of the expressed proteins. In addition, it is important to note that the degree of involucrin induction parallels the activation of *c-fos* expression (Fig. 7). The low level of *c-fos* induction and involucrin expression induced by CDK9 and cyclin T1 expression may due to the fact that BRD4, which is responsible for recruiting P-TEFB, is still being sequestered in BRD4-NUT foci. In conclusion, these experiments demonstrate that CBP and BRD4-P-TEFB can antagonize the sequestration effect of BRD4-NUT and stimulate *c-fos* transcription and NMC cellular differentiation.

DISCUSSION

NUT midline carcinoma is characterized as a poorly differentiated and highly aggressive cancer resulting from chromosomal translocation t(15;19)-induced in-frame fusion of the double bromodomain protein, BRD4, with the testis-specific NUT protein. The *BRD4-NUT* oncogenic fusion was first identified by French *et al.* (5) more than a decade ago; however, the molecular event that contributes to its oncogenic mechanism remains a subject of active investigation. In this study, we show that the BRD4-NUT fusion protein forms punctate foci in the HCC2429 NMC cancer cells as well as other cell lines such as C33A and 293T (Fig. 1 and supplemental Fig. S3). BRD4-NUT recruits HAT enzymes to induce histone hyperacetylation, which provide docking sites for accumulation of additional BRD4-NUT and BRD4 protein in these punctate chromatin foci. Through molecular interaction with BRD4, the P-TEFB transcriptional activation machinery is partially sequestered in the hyperacetylated and yet transcriptionally inactive chromatin foci (Fig. 4). This further limits the availability of transcriptional activators, including BRD4 and P-TEFB, at other transcription units such as the *c-fos* promoter, leading to the repression of *c-fos*, a BRD4-P-TEFB downstream gene and an important regulator of epithelial differentiation. These molecular events result in inhibition of cellular differentiation. Knockdown of the BRD4-NUT fusion expression disperses the transcriptionally inactive chromatin foci and releases the transcriptional activators to stimulate *c-fos*, leading to the restora-

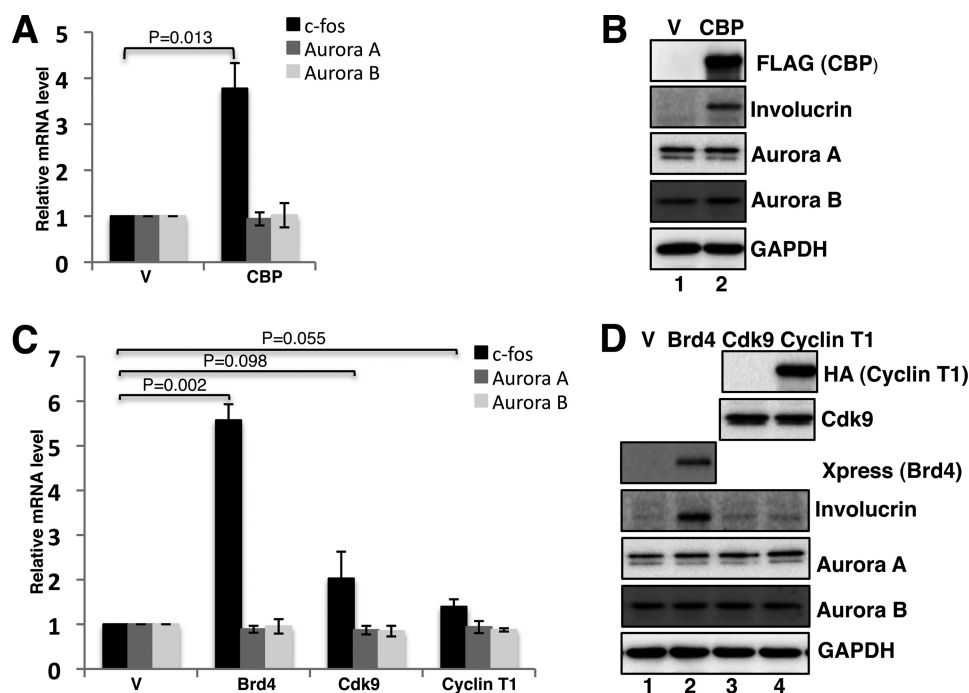


FIGURE 7. Expression of CBP and BRD4-P-TEFB stimulates *c-fos* transcription and cellular differentiation in NMC. *A*, HCC2429 cells were transfected with empty vector (V) or CBP expression construct. At 24 h post-transfection, RT-qPCR was performed to measure *c-fos*, *AURORA A*, and *AURORA B* mRNAs as described in Fig. 5*B*. Values represent the average of three independent experiments with *error bars* indicating standard deviation. *B*, HCC2429 cells were transfected as in *A*. At 48 h post-transfection, total cell lysates were analyzed by Western blot using indicated antibodies. *C*, HCC2429 cells were transfected with empty vector (V), Xpress-tagged BRD4, CDK9, or HA-cyclin T1 expression constructs. *c-fos*, *AURORA A*, and *AURORA B* mRNAs were measured and presented as in *A*. *D*, HCC2429 cells were transfected as in *C*. At 48 h post-transfection, total cell lysates were analyzed by Western blot using indicated antibodies. Xpress antibody was used to detect Xpress-tagged BRD4 expression in transfected cells.

tion of cellular differentiation signaling pathways. When CBP, BRD4, or P-TEFB is transiently expressed in HCC2429 cells to compensate for the lack of available transcriptional activators, *c-fos* transcription is stimulated, and cell differentiation is induced (Fig. 7). This study reveals a molecular model in which BRD4-NUT protein inhibits cellular differentiation and contributes to oncogenic progression by removing transcriptional activators from key genes such as *c-fos* to transcriptionally inactive BRD4-NUT foci. Our studies therefore provide additional insight into the molecular mechanism underlying the oncogenic activity of the BRD4-NUT fusion protein and how it may contribute to the poorly differentiated NMC morphology.

Although P-TEFB subunits CDK9 and cyclin T1 could be seen to accumulate at BRD4-NUT foci, the transcriptionally active markers, including RNAP II CTD serine 2 and serine 5 phosphorylation, are not present at these sites (Fig. 4). This indicates that although there is a high level of classical “activating” marks at these foci, including hyperacetylation of H3 and H4 as well as the recruitment of BRD4-P-TEFB, these foci are transcriptionally inactive. To our knowledge, transcriptionally inactive but hyperacetylated histone H3/H4 foci are a phenomenon unique to sperm development (50). The molecular basis for this transcriptional silencing despite histone hyperacetylation remains unknown and warrants further investigation.

Upon BRD4-NUT knockdown, the NMC cell line HCC2429 was shown to express the epithelial differentiation marker, involucrin, within 48 h. Consistent with the induction of cellular differentiation, *c-fos* mRNA expression increases substantially upon BRD4-NUT knockdown (Fig. 5, *B* and *C*). Depletion

of BRD4-NUT also leads to increased H4 acetylation and BRD4 recruitment on the *c-fos* promoter (Fig. 6). This result further supports that the BRD4-NUT fusion protein may normally repress *c-fos* expression through sequestering these important transcription activators. We have also examined the amount of P-TEFB present on the *c-fos* promoter and found that it is not significantly increased upon BRD4-NUT knockdown (data not shown). We reasoned that P-TEFB interacts with the *c-fos* promoter indirectly through BRD4 and is therefore physically located furthest away from the *c-fos* promoter. This could cause it to be poorly cross-linked with DNA in the ChIP experiment and lead to less efficient pull-down of its associated DNA. Because P-TEFB is normally kept in a functional equilibrium through alternately interacting with its positive regulator BRD4 and negative regulator, the HEXIM1 protein and 7SKsnRNA complex (51), it is also possible that a large amount of P-TEFB could exist in the inactive complex and only a very small portion of the BRD4-bound active form of P-TEFB is associated with the *c-fos* promoter. The amount of the active P-TEFB associated with the *c-fos* promoter may not be quantitatively measured by ChIP due to the low signal-to-noise ratio. To overcome this problem, we performed a ChIP experiment to specifically monitor the P-TEFB activity toward the RNAP II CTD serine 2 phosphorylation on the *c-fos* promoter. The ChIP data show that the CDK9-mediated RNAP II CTD serine 2 phosphorylation on the *c-fos* promoter was significantly increased upon BRD4-NUT knockdown (Fig. 6*A*), suggesting that depletion of BRD4-NUT could release the BRD4-P-TEFB

Perturbation of BRD4 Function in BRD4-NUT Carcinoma Cells

complex from the inactive chromatin foci to activate the *c-fos* promoter.

NUT expression is normally restricted to the testis. It is well established that in a variety of animal models, sperm chromatin undergoes extensive hyperacetylation just prior to exchange of core histones with sperm-specific chromatin proteins that aid in sperm nuclei compaction (50, 52, 53). In a previous study, Reynoird *et al.* (37) have reported that BRD4-NUT sequesters p300 to transcriptionally inactive histone-hyperacetylated chromatin domains. In addition to p300, we have found that other HATs such as GCN5 and TIP60 can also interact with NUT. These studies suggest that NUT might function by recruiting HAT enzymes to boost histone hyperacetylation during germ cell formation. It will be interesting to see what functional relevance these HATs might have in normal NUT function. However, the formation of histone-hyperacetylated foci could only be induced by the BRD4-NUT fusion protein; expression of the BRD4 short isoform or NUT protein separately did not recapitulate this phenotype (Fig. 2). This result suggests that anchoring the NUT moiety to the acetylated histone through the double bromodomains is required for this event. The region of the fusion protein responsible for inducing histone hyperacetylation on chromatin foci could be assigned to the NUT moiety, specifically the region between amino acids 300 and 550 (supplemental Fig. S5). Together, our studies demonstrate how the off-context expression of a testis-specific factor upon fusion to the BRD4 moiety could lead to severe changes in fundamental cellular processes and contribute to the development of a highly aggressive carcinoma.

The BRD4-NUT fusion represents both a gain and loss of function for the *BRD4* gene. The fusion of NUT generally deletes the C-terminal domain of BRD4 required for P-TEF β binding and activation; therefore, BRD4-NUT cannot participate in transcriptional activation through P-TEF β . BRD4 clearly gains a histone acetylation function through fusion with the NUT protein, which recruits HATs.

Our study demonstrates the functional importance of BRD4-mediated transcriptional activation and how its aberrant recruitment to transcriptionally inactive chromatin foci can have profound implications for cellular functions. The inhibition of cellular transcriptional activation caused by BRD4-NUT might have a broad effect on cellular gene expression profiles, which might include genes important for cell proliferation, metastasis, or invasiveness. Therefore, a genome-wide microarray analysis might be helpful to identify other abnormally expressed genes. Poorly differentiated or undifferentiated cancers are classified as high grade with more rapid growth and faster spread than tumors with a lower grade (54). How blocking cellular differentiation can contribute to cancer development remains an interesting question for future investigation.

BRD4 activation in human breast carcinomas induces a gene expression signature that efficiently predicts survival, establishing that dysregulation of BRD4-associated pathways may play an important role in breast cancer progression (49). The cancer-predisposing genetic mutation in the t(15;19) carcinoma hence provides a novel tool to further probe the mechanisms by which BRD4-NUT perturbs BRD4 cellular functions to achieve malignant progression. These studies serve as a starting point

for unraveling the complex BRD4 cellular function in global genome reorganization during tumorigenesis and epithelial differentiation. By examining the structural and functional consequences associated with the t(15;19)-mediated juxtaposition of *BRD4* to *NUT*, this study starts to uncover the mechanism underlying the neoplastic activity of the *BRD4-NUT* fusion oncogene that accounts for this highly lethal carcinoma. The outcome of future studies on this subject will offer promising leads for developing efficient therapeutic strategies to antagonize NMC tumorigenesis.

Acknowledgments—We thank the members of our laboratory for helpful discussions, Dr. Thao P. Dang (Vanderbilt University) for providing HCC2429 cell lines and GFP-BRD4-NUT expression construct, and Dr. Bassel E. Sawaya (Temple University) for providing P-TEF β expression constructs.

REFERENCES

1. Mitelman, F., Johansson, B., and Mertens, F. (2007) *Nat. Rev. Cancer* **7**, 233–245
2. Brenner, J. C., and Chinnaiyan, A. M. (2009) *Biochim. Biophys. Acta* **1796**, 201–215
3. Edwards, P. A. (2010) *J. Pathol.* **220**, 244–254
4. Teixeira, M. R. (2006) *Crit. Rev. Oncog.* **12**, 257–271
5. French, C. A., Miyoshi, I., Aster, J. C., Kubonishi, I., Kroll, T. G., Dal Cin, P., Vargas, S. O., Perez-Atayde, A. R., and Fletcher, J. A. (2001) *Am. J. Pathol.* **159**, 1987–1992
6. French, C. A., Miyoshi, I., Kubonishi, I., Grier, H. E., Perez-Atayde, A. R., and Fletcher, J. A. (2003) *Cancer Res.* **63**, 304–307
7. Haruki, N., Kawaguchi, K. S., Eichenberger, S., Massion, P. P., Gonzalez, A., Gazdar, A. F., Minna, J. D., Carbone, D. P., and Dang, T. P. (2005) *J. Med. Genet.* **42**, 558–564
8. Dey, A., Chitsaz, F., Abbasi, A., Misteli, T., and Ozato, K. (2003) *Proc. Natl. Acad. Sci. U.S.A.* **100**, 8758–8763
9. Dey, A., Ellenberg, J., Farina, A., Coleman, A. E., Maruyama, T., Sciortino, S., Lippincott-Schwartz, J., and Ozato, K. (2000) *Mol. Cell. Biol.* **20**, 6537–6549
10. Dey, A., Nishiyama, A., Karpova, T., McNally, J., and Ozato, K. (2009) *Mol. Biol. Cell* **20**, 4899–4909
11. Houzelstein, D., Bullock, S. L., Lynch, D. E., Grigorieva, E. F., Wilson, V. A., and Beddington, R. S. (2002) *Mol. Cell. Biol.* **22**, 3794–3802
12. Maruyama, T., Farina, A., Dey, A., Cheong, J., Bermudez, V. P., Tamura, T., Sciortino, S., Shuman, J., Hurwitz, J., and Ozato, K. (2002) *Mol. Cell. Biol.* **22**, 6509–6520
13. Mochizuki, K., Nishiyama, A., Jang, M. K., Dey, A., Ghosh, A., Tamura, T., Natsume, H., Yao, H., and Ozato, K. (2008) *J. Biol. Chem.* **283**, 9040–9048
14. Nishiyama, A., Dey, A., Miyazaki, J., and Ozato, K. (2006) *Mol. Biol. Cell* **17**, 814–823
15. Yang, Z., He, N., and Zhou, Q. (2008) *Mol. Cell. Biol.* **28**, 967–976
16. You, J., Li, Q., Wu, C., Kim, J., Ottinger, M., and Howley, P. M. (2009) *Mol. Cell. Biol.* **29**, 5094–5103
17. Jang, M. K., Mochizuki, K., Zhou, M., Jeong, H. S., Brady, J. N., and Ozato, K. (2005) *Mol. Cell* **19**, 523–534
18. Yang, Z., Yik, J. H., Chen, R., He, N., Jang, M. K., Ozato, K., and Zhou, Q. (2005) *Mol. Cell* **19**, 535–545
19. You, J., Croyle, J. L., Nishimura, A., Ozato, K., and Howley, P. M. (2004) *Cell* **117**, 349–360
20. Ottinger, M., Christalla, T., Nathan, K., Brinkmann, M. M., Viejo-Borbolla, A., and Schulz, T. F. (2006) *J. Virol.* **80**, 10772–10786
21. You, J., Srinivasan, V., Denis, G. V., Harrington, W. J., Jr., Ballestas, M. E., Kaye, K. M., and Howley, P. M. (2006) *J. Virol.* **80**, 8909–8919
22. Bisgrove, D. A., Mahmoudi, T., Henklein, P., and Verdin, E. (2007) *Proc. Natl. Acad. Sci. U.S.A.* **104**, 13690–13695
23. Cho, W. K., Zhou, M., Jang, M. K., Huang, K., Jeong, S. J., Ozato, K., and

- Brady, J. N. (2007) *J. Virol.* **81**, 11179–11186
24. Lin, A., Wang, S., Nguyen, T., Shire, K., and Frappier, L. (2008) *J. Virol.* **82**, 12009–12019
25. Schweiger, M. R., Ottinger, M., You, J., and Howley, P. M. (2007) *J. Virol.* **81**, 9612–9622
26. Schweiger, M. R., You, J., and Howley, P. M. (2006) *J. Virol.* **80**, 4276–4285
27. Smith, J. A., White, E. A., Sowa, M. E., Powell, M. L., Ottinger, M., Harper, J. W., and Howley, P. M. (2010) *Proc. Natl. Acad. Sci. U.S.A.* **107**, 3752–3757
28. Wu, S. Y., Lee, A. Y., Hou, S. Y., Kemper, J. K., Erdjument-Bromage, H., Tempst, P., and Chiang, C. M. (2006) *Genes Dev.* **20**, 2383–2396
29. French, C. A., Kutok, J. L., Faquin, W. C., Toretsky, J. A., Antonescu, C. R., Griffin, C. A., Nose, V., Vargas, S. O., Moschovi, M., Tzortzatou-Stathopoulou, F., Miyoshi, I., Perez-Atayde, A. R., Aster, J. C., and Fletcher, J. A. (2004) *J. Clin. Oncol.* **22**, 4135–4139
30. Engleson, J., Soller, M., Panagopoulos, I., Dahlén, A., Dictor, M., and Jerkeman, M. (2006) *BMC Cancer* **6**, 69
31. Mertens, F., Wiebe, T., Adlercreutz, C., Mandahl, N., and French, C. A. (2007) *Pediatr. Blood Cancer* **49**, 1015–1017
32. Stelow, E. B., Bellizzi, A. M., Taneja, K., Mills, S. E., Legallo, R. D., Kutok, J. L., Aster, J. C., and French, C. A. (2008) *Am. J. Surg. Pathol.* **32**, 828–834
33. den Bakker, M. A., Beverloo, B. H., van den Heuvel-Eibrink, M. M., Meeuwis, C. A., Tan, L. M., Johnson, L. A., French, C. A., and van Leenders, G. J. (2009) *Am. J. Surg. Pathol.* **33**, 1253–1258
34. French, C. A. (2010) *J. Clin. Pathol.* **63**, 492–496
35. Ziai, J., French, C. A., and Zambrano, E. (2010) *Head Neck Pathol.* **4**, 163–168
36. French, C. A., Ramirez, C. L., Kolmakova, J., Hickman, T. T., Cameron, M. J., Thyne, M. E., Kutok, J. L., Toretsky, J. A., Tadarvarthy, A. K., Kees, U. R., Fletcher, J. A., and Aster, J. C. (2008) *Oncogene* **27**, 2237–2242
37. Reynoird, N., Schwartz, B. E., Delvecchio, M., Sadoul, K., Meyers, D., Mukherjee, C., Caron, C., Kimura, H., Rousseaux, S., Cole, P. A., Panne, D., French, C. A., and Khochbin, S. (2010) *EMBO J.* **29**, 2943–2952
38. Filippakopoulos, P., Qi, J., Picaud, S., Shen, Y., Smith, W. B., Fedorov, O., Morse, E. M., Keates, T., Hickman, T. T., Felletar, I., Philpott, M., Munro, S., McKeown, M. R., Wang, Y., Christie, A. L., West, N., Cameron, M. J., Schwartz, B., Heightman, T. D., La Thangue, N., French, C. A., Wiest, O., Kung, A. L., Knapp, S., and Bradner, J. E. (2010) *Nature* **468**, 1067–1073
39. Eckert, R. L., Crish, J. F., and Robinson, N. A. (1997) *Physiol. Rev.* **77**, 397–424
40. Okada, Y., Senba, E., Shirai, K., Ueyama, T., Reinach, P., and Saika, S. (2008) *Jpn. J. Ophthalmol.* **52**, 1–7
41. Rorke, E. A., Adhikary, G., Jans, R., Crish, J. F., and Eckert, R. L. (2010) *Oncogene* **29**, 5873–5882
42. Birek, C., Lui, E., and Dardick, I. (1993) *Am. J. Pathol.* **142**, 917–923
43. Klimpfinger, M., Zisser, G., Ruhri, C., Pütz, B., Steindorfer, P., and Höfler, H. (1990) *Virchows Arch. B Cell Pathol. Incl. Mol. Pathol.* **59**, 165–171
44. Lee, H. Y., Chaudhary, J., Walsh, G. L., Hong, W. K., and Kurie, J. M. (1998) *Oncogene* **16**, 3039–3046
45. Levin, W. J., Press, M. F., Gaynor, R. B., Sukhatme, V. P., Boone, T. C., Reissmann, P. T., Figlin, R. A., Holmes, E. C., Souza, L. M., and Slamon, D. J. (1995) *Oncogene* **11**, 1261–1269
46. Milde-Langosch, K., Kappes, H., Riethdorf, S., Löning, T., and Bamberger, A. M. (2003) *Breast Cancer Res. Treat.* **77**, 265–275
47. Yan, J., Li, Q., Lievens, S., Tavernier, J., and You, J. (2010) *J. Virol.* **84**, 76–87
48. Byun, J. S., Wong, M. M., Cui, W., Idelman, G., Li, Q., De Siervi, A., Bilke, S., Haggerty, C. M., Player, A., Wang, Y. H., Thirman, M. J., Kaberlein, J. J., Petrovas, C., Koup, R. A., Longo, D., Ozato, K., and Gardner, K. (2009) *Proc. Natl. Acad. Sci. U.S.A.* **106**, 19286–19291
49. Crawford, N. P., Alsarraj, J., Lukes, L., Walker, R. C., Officewala, J. S., Yang, H. H., Lee, M. P., Ozato, K., and Hunter, K. W. (2008) *Proc. Natl. Acad. Sci. U.S.A.* **105**, 6380–6385
50. Hazzouri, M., Pivot-Pajot, C., Faure, A. K., Usson, Y., Pelletier, R., Sèle, B., Khochbin, S., and Rousseaux, S. (2000) *Eur. J. Cell Biol.* **79**, 950–960
51. Zhou, Q., and Yik, J. H. (2006) *Microbiol. Mol. Biol. Rev.* **70**, 646–659
52. Boussouar, F., Rousseaux, S., and Khochbin, S. (2008) *Cell Cycle* **7**, 3499–3502
53. Pivot-Pajot, C., Caron, C., Govin, J., Vion, A., Rousseaux, S., and Khochbin, S. (2003) *Mol. Cell. Biol.* **23**, 5354–5365
54. American Joint Committee on Cancer (2002) *AJCC Cancer Staging Manual*, 6th Ed., Springer-Verlag, Inc., New York